

Current-Induced Effects in Nanoscale Conductors

Neil Bushong* and Massimiliano Di Ventra†

Department of Physics, University of California, San Diego, La Jolla, CA 92093-0319

We present an overview of current-induced effects in nanoscale conductors with emphasis on their description at the atomic level. In particular, we discuss steady-state current fluctuations, current-induced forces, inelastic scattering and local heating. All of these properties are calculated in terms of single-particle wavefunctions computed using a scattering approach within the static density-functional theory of many-electron systems. Examples of current-induced effects in atomic and molecular wires will be given and comparison with experimental results will be provided when available.

CURRENT THROUGH A NANOSCALE JUNCTION

Transport of electrical charge across a nanoscale junction is accompanied by many effects, such as fluctuations of the average current; transfer of energy between electrons and ions and consequent heating of the junction; and forces on ions due to current-induced variations of the electronic distribution [1]. In this work we will discuss these effects separately, and we will focus on their description at the atomic level. It is, however, important to realize that there has to be a (yet unknown) relation between these different properties. Such relation would constitute an important contribution to our understanding of transport in nanoscale systems.

The static scattering approach to electrical conduction will be the underlying theme of this review. However, we point out that novel time-dependent formulations of the transport problem may lead us to a better understanding of these effects [2, 3]. In what follows we picture a nanoscale junction as formed by two semi-infinite electrodes held a fixed distance apart, with a nanoscale object bridging the gap between them. The nanoscale object could be a single atom, a chain of atoms, a molecule, or any system with nanoscale dimensions [4, 5, 6, 7, 8, 9, 10, 11, 12, 13, 14, 15, 16]. We then consider the problem of DC current flow from one electrode to the other as the result of an applied bias V_B . If we take the left electrode to be positively biased, electrons will flow from the right electrode to the left one. A buildup of negative charge will be present on the surface of the right electrode within a screening length of the electrode surface. Similarly, a buildup of positive charge will exist on the surface of the left electrode due to a corresponding depletion of electrons [14, 15]. We will assume that, far away from the junction, the electrons in each electrode are in local thermal equilibrium and their statistics are described by the Fermi-Dirac distribution, so that $V_B = E_{FR} - E_{FL}$, where $E_{FL(R)}$ is the chemical potential deep in the left (right) electrode. (Here, as in the rest of this work, we use atomic units.)

We calculate the transport properties of this system by expanding the stationary states of the Hamiltonian

into a set of left- and right-moving waves. We then sum each left- and right-moving state, weighting them with a Fermi function according to their energy. The stationary scattering states of the bare electrodes have the form

$$\Psi_{E\mathbf{K}_{\parallel}}^0(\mathbf{r}) = e^{i\mathbf{K}_{\parallel} \cdot \mathbf{Y}} u_{E\mathbf{K}_{\parallel}}(z), \quad (1)$$

with the following boundary conditions [17]:

$$u_{E\mathbf{K}_{\parallel}}(z) = (2\pi)^{3/2} k_R^{-1/2} \times \begin{cases} e^{-ik_R z} + R e^{ik_R z}, & z \rightarrow \infty \\ T e^{-ik_L z}, & z \rightarrow -\infty. \end{cases} \quad (2)$$

\mathbf{K}_{\parallel} is the electron momentum in the plane parallel to the electrode surfaces. We have defined $\frac{1}{2}k_R^2 = E - \frac{1}{2}|\mathbf{K}_{\parallel}|^2 - v_{eff}(\infty)$, and $\frac{1}{2}k_L^2 = E - \frac{1}{2}|\mathbf{K}_{\parallel}|^2 - v_{eff}(-\infty)$. \mathbf{Y} is the component of the position vector in a plane parallel to the electrode surfaces, and z is the coordinate perpendicular to them. $v_{eff}(\pm\infty)$ is the bottom of the electronic energy band deep within the right/left electrode. The wavefunctions Ψ^0 satisfy the continuum normalization condition

$$\int d^3\mathbf{r} [\Psi_{E'\mathbf{K}'_{\parallel}}^0(\mathbf{r})]^* \Psi_{E\mathbf{K}_{\parallel}}^0(\mathbf{r}) = \delta(E' - E) \delta(\mathbf{K}'_{\parallel} - \mathbf{K}_{\parallel}). \quad (3)$$

Since the details of the electrodes are not important up to the interface with the sample, we represent them using a uniform-background (jellium) model [14, 15]. The potential V the electrons experience when they scatter through the nanojunction is [59]

$$V(\mathbf{r}, \mathbf{r}') = v_{ps}(\mathbf{r}, \mathbf{r}') + \left[v_{xc}[n(\mathbf{r})] - v_{xc}[n^0(\mathbf{r})] + \int d^3\mathbf{r}'' \frac{\delta n(\mathbf{r}'')}{|\mathbf{r} - \mathbf{r}''|} \right] \delta(\mathbf{r} - \mathbf{r}'). \quad (4)$$

The term v_{ps} is the electron-ion interaction potential that we represent with (nonlocal) pseudopotentials; v_{xc} is the exchange-correlation potential computed using the local-density approximation to density functional theory (DFT) [60]; $n^0(\mathbf{r})$ is the electronic density for the pair of biased bare electrodes; $n(\mathbf{r})$ is the electronic density for the total system, and $\delta n(\mathbf{r})$ is their difference. We are implicitly assuming that static DFT gives a reasonable account of the scattering properties of a nanoscale

system, at least in linear response. While this may be true for metallic junctions it is not obvious for molecular junctions [18]. However, in linear response and far from the resonant regime, we expect basic physical trends for these systems to be reproduced well by static DFT [18].

The full Hamiltonian of the system is $H = H_0 + V$, where H_0 is the Hamiltonian due to the bare biased electrodes, and V is the scattering potential. Our next task is to find the self-consistent solutions to the equation $H\Psi_E = E\Psi_E$, which we can put into the Lippmann-Schwinger form:

$$\Psi_{E\mathbf{K}_{\parallel}}(\mathbf{r}) = \Psi_{E\mathbf{K}_{\parallel}}^0(\mathbf{r}) + \int d^3\mathbf{r}' d^3\mathbf{r}'' G_E^0(\mathbf{r}, \mathbf{r}') V(\mathbf{r}', \mathbf{r}'') \Psi_{E\mathbf{K}_{\parallel}}(\mathbf{r}''). \quad (5)$$

The quantity G_E^0 is the Green's function for the bare electrodes, and needs to be calculated for each energy E .

Lastly, the total density of the system is

$$n(\mathbf{r}) = 2 \sum_i |\Psi_i(\mathbf{r})|^2 + 2 \int dE \int d^2\mathbf{K}_{\parallel} |\Psi_{E\mathbf{K}_{\parallel}}(\mathbf{r})|^2, \quad (6)$$

where we have included a factor of 2 due to spin degeneracy. The Ψ_i 's are the bound states of H , if any exist. They can be calculated by direct diagonalization of the full Hamiltonian H . In order to find a self-consistent solution for the density, equations (4), (5) and (6) are solved iteratively.

One has the freedom to choose a basis set to represent the wave functions. Due to the non-variational nature of the electrical current, the issue of which basis set to use in a given calculation is far from trivial [19]. In the examples that follow, plane waves have been used as basis set [61], which allows easy testing of the convergence of the results [19].

Once the wavefunctions have been calculated self-consistently, the total electric current density (at zero temperature) is given by

$$\mathbf{j}(\mathbf{r}) = -2 \int_{E_{\text{FL}}}^{E_{\text{FR}}} dE \int d^2\mathbf{K}_{\parallel} \text{Im}\{[\Psi_{E\mathbf{K}_{\parallel}}(\mathbf{r})]^* \nabla \Psi_{E\mathbf{K}_{\parallel}}(\mathbf{r})\}. \quad (7)$$

The quantity we are interested in is the extra current δJ due to presence of the nanojunction [20, 21, 22, 23] (two semi-infinite contacts have infinite surface area, and thus pass infinite current)

$$\delta J = \int d^2\mathbf{Y} \hat{z} \cdot [\mathbf{j}(\mathbf{r}) - \mathbf{j}^0(\mathbf{r})], \quad (8)$$

where \mathbf{j} is the electric current density, and we have defined \mathbf{j}^0 to be the current density in the absence of the nanojunction. The current defined in equation (8) is the average current that flows across the nanojunction. Fluctuations with respect to that average are expected and will be described later in this work.

It is worth noting that, in contrast to references [24, 25, 26, 27], we do not calculate the electrical current using any of the Landauer formulas [28, 29]; rather, the current is calculated as the expectation value of the current operator over single-particle states. Clearly, it can be proven that when the transmission probabilities are extracted from the single-particle scattering wavefunctions, we recover from equation (8) the conventional two-probe Landauer formula [30].

CURRENT-INDUCED FORCES

Now that we have computed the stationary scattering states and corresponding current we can look at one of the effects induced by electron flow. We first focus on current-induced forces, i.e. the phenomenon by which atoms in a current-carrying wire are subject to forces due to the local change in self-consistent electronic distribution [31, 32]. There are several open questions related to current-induced forces, the most notable of which is their conservative nature [33]. Here we will focus on their dependence on some microscopic properties. We will show that these forces are a non-linear function of the junction properties, such as its current density, charge density and length.

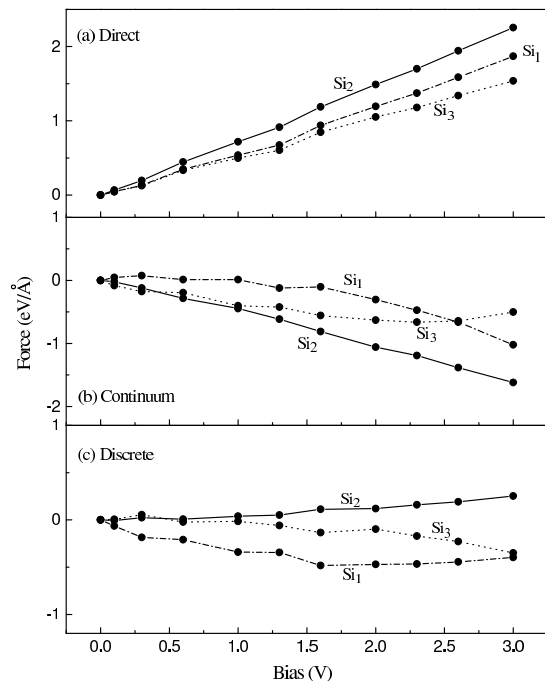


FIG. 1: Different contributions to the total force for each of the three atoms composing a silicon wire, as a function of bias. See text for details. Reprinted figure with permission from [34]. Copyright 2003 by the American Physical Society.

Let us first define forces in a current-carrying wire. We first note that in this non-equilibrium problem the

usual Hellman-Feynmann theorem is not valid [31, 33]. A meaningful definition of force on ions can then be obtained by either the classical limit of Ehrenfest's theorem applied to the rate of change of ionic momentum [31] or from the Euler-Lagrange equation of motion for the classical ions [35]. Both approaches yield the same expression for the force on an ion, with position \mathbf{R} , due to the self-consistent electronic density $\rho(\mathbf{r})$ under current flow [35],

$$\mathbf{F} = - \int d\mathbf{r} \frac{\partial v_{\text{ps}}}{\partial \mathbf{R}} \rho(\mathbf{r}), \quad (9)$$

which can be equivalently written as [31]

$$\mathbf{F} = - \sum_i \left\langle \psi_i \left| \frac{\partial v_{\text{ps}}}{\partial \mathbf{R}} \right| \psi_i \right\rangle - \lim_{\Delta \rightarrow 0} \int_{\sigma} dE \left\langle \psi_{\Delta} \left| \frac{\partial v_{\text{ps}}}{\partial \mathbf{R}} \right| \psi_{\Delta} \right\rangle. \quad (10)$$

The first term on the RHS of Eq. (10) is similar to the usual Hellmann-Feynman contribution to the force due to localized electronic states $|\psi_i\rangle$. The second term is the contribution due to continuum states [31]. The wavefunctions $|\psi_{\Delta}\rangle$ are eigendifferentials for each energy interval Δ in the continuum σ [31]. Finally, an additional contribution from ion-ion interactions needs to be taken into account.

For convenience we can separate the total force into two contributions. We define “direct force” to be the portion of the total force due to the charge distribution of the biased bare electrodes. We then call the remaining term the “electron wind force” [62]. There exists an inelastic portion of the electron wind force due to energy transfer from electrons to ions, in the form of phonon excitations; however, this contribution is generally negligible compared to the elastic one and will be neglected here [34].

We note that atomic relaxations induced by current flow do not have a large effect on the absolute value of the current that passes through the junction, even in the limit of high voltages and current densities [31, 34, 36, 37]. While this result says nothing about the mechanical stability of current-carrying wires under bias, it allows us to study several transport properties assuming atomic positions fixed at their zero bias value.

Let us now look at the dependence of these forces on microscopic details. As an example, in Figure 1 we consider a nanoscopic wire composed of three silicon atoms between two bulk electrodes. We keep atomic positions fixed at their zero bias values. For each atom in the junction, we plot the direct force, the electron wind force due to the continuum states, and the electron wind force due to the discrete part of the spectrum.

The direct force is almost linear with applied bias, with the force on the central atom being the largest. Closer to the electrode surfaces, the electrostatic potential ceases to be a linear function of position, causing the force on the other two atoms to be slightly smaller. Note that the force on the central atom due to states in the continuum

is positive (i.e. pushes the atom to the left, in the same direction as the electron flow). However, the force on the central atom due to states in the discrete spectrum is almost zero, even at larger biases. The reason for this behavior is that the amount of charge localized around the central atom is almost constant in the applied bias, and so the corresponding force is also constant [34].

Figure 2(a) through (c) shows the force on specific atoms in silicon wires composed of varying numbers of atoms, while Figure 2(d) shows the average force on the total wires. It is difficult to extract overall trends from Figures 2(a) through (c), although it is interesting to note that the second atom from the left (labeled Si_2) is consistently the atom that experiences the greatest force. Figure 2(d), however, follows an obvious trend: the average force saturates with increasing number of atoms. This comes from the fact that, as the length of the wire increases, the boundary effects due to the electrodes become less important. This result suggests that longer

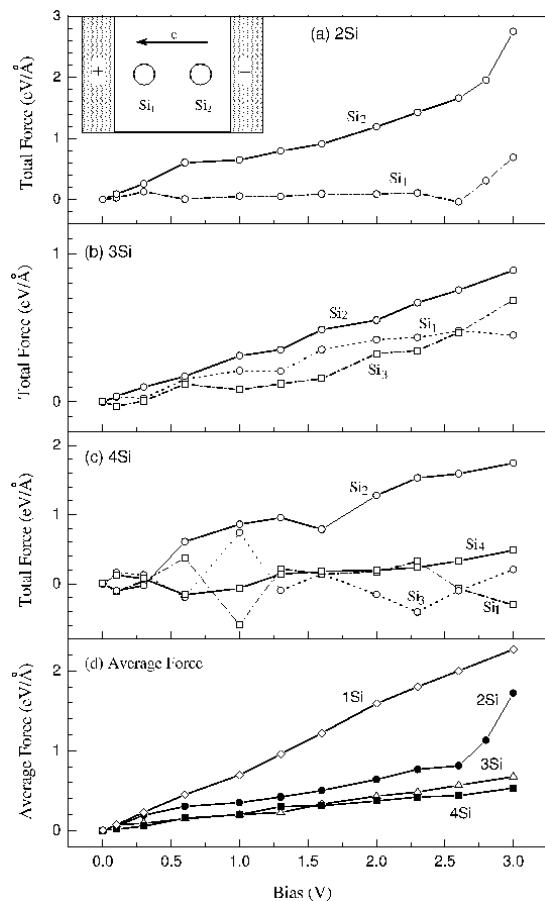


FIG. 2: Total force on each atom in atomic wires consisting of (a) two, (b) three, and (c) four silicon atoms. The inset shows a schematic of the wire that is composed of two silicon atoms. (d) The average force on each wire. Reprinted figure with permission from [34]. Copyright 2003 by the American Physical Society.

wires are more difficult to break under current flow, an important factor to consider in nanoscale devices.

SHOT NOISE

In this section we will discuss steady-state current fluctuations that occur due to the quantization of charge. Shot noise is quite distinct from (equilibrium) thermal noise and is generally unavoidable, even at zero temperature [38].

We will first derive an expression of shot noise in terms of single-particle wavefunctions. In order to do so, let us write the field operator for electrons $\hat{\Psi}$ as combination of a field operator due to electrons incident from the left, and one due to electrons incident from the right [30, 39]

$$\hat{\Psi} = \hat{\Psi}^L + \hat{\Psi}^R. \quad (11)$$

We can further expand each of these field operators into the single particle wave functions (5):

$$\hat{\Psi}^{L(R)} = \sum_E e^{-i\omega t} a_E^{L(R)} \Psi_E^{L(R)}(\mathbf{r}, \mathbf{K}_{\parallel}). \quad (12)$$

Again, we have used \mathbf{K}_{\parallel} to denote the component of the electron's incident momentum that is parallel to the surfaces of the electrodes [63].

The coefficients $a_E^{L(R)}$ are the annihilation operators for electrons incident from the left (right) reservoir. These operators satisfy the usual anticommutation relation $\{a_E^{\phi}, a_{E'}^{\chi\dagger}\} = \delta_{\phi\chi} \delta(E - E')$, where $\phi, \chi = R, L$. We will again assume that the electrons coming from the left (right) reservoir are in local thermal equilibrium at a temperature T_e far away from the junction, so that their statistics are given by the Fermi-Dirac distribution function $f_E^{L(R)}$, i.e.

$$\langle a_E^{\phi\dagger} a_{E'}^{\chi} \rangle = \delta_{\phi\chi} \delta(E - E') f_E^{\phi} \quad (13)$$

$$= \frac{\delta_{\phi\chi} \delta(E - E')}{e^{[E - E_{F\phi}]/k_B T_e} + 1}. \quad (14)$$

Using the field operator (11), we can define the current operator

$$\hat{I}(z, t) = -i \int d\mathbf{Y} \int d\mathbf{K}_{\parallel} (\hat{\Psi}^{\dagger} \partial_z \hat{\Psi} - \partial_z \hat{\Psi}^{\dagger} \hat{\Psi}). \quad (15)$$

In the limit of zero temperature, the Fermi distribution reduces to a step function; if we again assume the chemical potential in the right reservoir E_{FR} is higher than the chemical potential in the left reservoir E_{FL} , then at zero temperature the average value of the current is just

$$\langle \hat{I} \rangle = -i \int_{E_{FL}}^{E_{FR}} dE \int d\mathbf{Y} \int d\mathbf{K}_{\parallel} \tilde{I}_{E,E}^{R,R}, \quad (16)$$

where

$$\tilde{I}_{E,E'}^{\phi,\chi} = (\Psi_E^{\phi})^* \nabla \Psi_{E'}^{\chi} - \nabla (\Psi_E^{\phi})^* \Psi_{E'}^{\chi}, \quad (17)$$

and $*$ denotes complex conjugation.

We define shot noise as the Fourier transform of the electric current autocorrelation function in the limit of zero frequency and zero temperature [38, 40]:

$$2\pi S(\omega) = \int dt e^{i\omega t} \langle \Delta \hat{I}(t) \Delta \hat{I}(0) \rangle, \quad (18)$$

where the excess current operator $\Delta \hat{I}(t)$ is equal to $\hat{I}(t) - \langle \hat{I} \rangle$. The evaluation of this expression is quite cumbersome and therefore we do not include it here. We only mention that we need to evaluate terms of the form $\langle \hat{A}_4 \hat{A}_3 \hat{A}_2 \hat{A}_1 \rangle$, where the \hat{A}_i 's are raising and lowering operators. We can evaluate these terms with the Bloch-De Dominicis theorem [41]:

$$\begin{aligned} \langle \hat{A}_4 \hat{A}_3 \hat{A}_2 \hat{A}_1 \rangle &= \langle \hat{A}_4 \hat{A}_3 \rangle \langle \hat{A}_2 \hat{A}_1 \rangle + \eta \langle \hat{A}_4 \hat{A}_2 \rangle \langle \hat{A}_3 \hat{A}_1 \rangle \\ &\quad + \eta^2 \langle \hat{A}_4 \hat{A}_1 \rangle \langle \hat{A}_3 \hat{A}_2 \rangle, \end{aligned} \quad (19)$$

where $\eta = -1$ for fermions, and $+1$ for bosons. The end result is

$$\begin{aligned} S(\omega) &= \sum_{\phi, \chi=L,R} \int dE f_{E+\omega}^{\phi} (1 - f_E^{\chi}) \int d\mathbf{Y}_1 \int d\mathbf{K}_1 \\ &\quad \times \tilde{I}_{E+\omega,E}^{\phi\chi} \int d\mathbf{Y}_2 \int d\mathbf{K}_2 \tilde{I}_{E,E+\omega}^{\chi\phi}. \end{aligned} \quad (20)$$

In the limit of zero frequency and zero temperature, equation (20) reduces to [30, 39]

$$S = \int_{E_{FL}}^{E_{FR}} dE \left| \int d\mathbf{R} \int d\mathbf{K} \tilde{I}_{E,E}^{LR} \right|^2. \quad (21)$$

This is the desired expression relating shot noise to single-particle wavefunctions [64].

In the case of uncorrelated electrons, the magnitude of the shot noise becomes $S_P = 2eI$, where e is the electron charge, and I is the dc current. This corresponds to the noise of a series of incident particles, the time between the arrivals of which follows a Poissonian distribution function. For this reason, S_P is sometimes called the Poisson value for the shot noise [38, 42]. In general, however, the magnitude of the shot noise will be less than the Poisson value. A relative measure of noise is therefore the Fano factor F , defined as the ratio between shot noise S and the Poisson limit S_P .

We are now ready to discuss an example of noise properties of a nanoscale junction. We again look at the properties of a junction formed by a short wire of silicon atoms between two bulk electrodes. Other examples of noise in atomic-scale systems can be found in references [39] and [30].

Figure 3 shows the results of conductance and Fano factor for such a system for a bias of 0.01 V. We first notice that the Fano factor is strongly nonlinear as a function of bias. It is also considerably enhanced for very short wires due to the large contribution from the metal

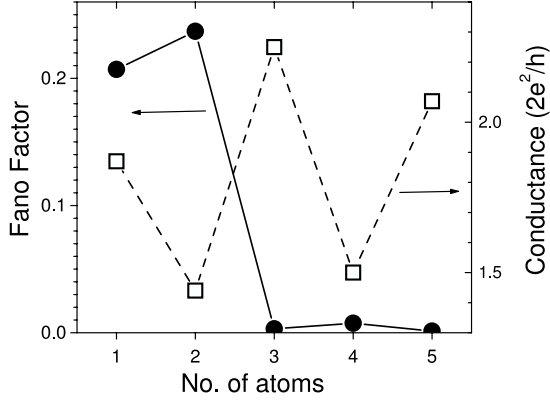


FIG. 3: Fano factor and conductance for a nanojunction composed of different numbers of silicon atoms. Reprinted figure with permission from [39]. Copyright 2003 by the American Physical Society.

electrodes. In addition, the Fano factor oscillates as a function of number of silicon atoms. The conductance shows a similar but opposite oscillatory trend. Both the noise and conductance oscillations are due to the fact that a Si wire made up of an even number of atoms has fully-occupied π orbitals, while a wire made up of an odd number of atoms has a half-filled π state at the Fermi level [43].

Other interesting properties of shot noise in nanoscale systems include its dependence on contact geometry and interwire interactions [30]. We refer the reader to the original papers for a discussion of these effects.

LOCAL HEATING

Local heating occurs when electrons in a current-carrying wire exchange energy with phonons [44, 45, 46, 47, 48]. Accordingly, there are four main processes that contribute to local heating in the junction:

1. Cooling processes in which an electron incident from the left absorbs a phonon, which we will denote by the superscript L, 1;
2. Heating processes in which an electron incident from the left emits a phonon, denoted by the superscript L, 2;
3. Cooling processes in which an electron incident from the right absorbs a phonon, denoted by the superscript R, 1; and
4. Heating processes in which an electron incident from the right emits a phonon, denoted by the superscript R, 2.

The power generated in a nanoscale junction is given by the sum of the average power generated by those four

processes, summed over all possible vibrational modes:

$$W_{\text{tot}}^{\text{avg.}} = \sum_{\text{vib. modes}} (\langle W^{\text{R},2} \rangle + \langle W^{\text{L},2} \rangle - \langle W^{\text{R},1} \rangle - \langle W^{\text{L},1} \rangle) \quad (22)$$

In addition to the above processes, cooling occurs due to dissipation of energy in the bulk electrodes [65]. In order to evaluate the power generated by each of those processes, we first need to consider the full many-body Hamiltonian of the system:

$$H = H_{\text{el}} + H_{\text{ion}} + H_{\text{el-ion}} \quad (23)$$

Here, H_{el} is the electronic Hamiltonian (including electron-electron effects), H_{ion} is the ionic Hamiltonian, given by

$$H_{\text{ion}} = \sum_{i=1}^N \frac{\mathbf{P}_i^2}{2M_i} + \sum_{i,j} V_{\text{ion}}(\mathbf{R}_i - \mathbf{R}_j), \quad (24)$$

and $H_{\text{el-ion}}$ is the electron-ion interaction,

$$H_{\text{el-ion}} = \sum_{i,j} V_{\text{el-ion}}(\mathbf{r}_i - \mathbf{R}_j). \quad (25)$$

\mathbf{P}_i , M_i and \mathbf{R}_i denote the momentum, mass and position of the i^{th} ion (out of a total of N ions), while \mathbf{r}_i denotes the position of the i^{th} electron.

We assume that each ion executes a small vibration about its equilibrium position \mathbf{R}_j^0 so that its displacement is given by $\mathbf{Q}_j = \mathbf{R}_j - \mathbf{R}_j^0$. We can decouple these ionic vibrations by introducing normal coordinates $\{q_{j\beta}\}$ so that the α^{th} component ($\alpha = x, y, z$) of \mathbf{Q}_i is given by

$$(\mathbf{Q}_i)_\alpha = \sum_{j=1}^N \sum_{\beta=1}^3 A_{i\alpha,j\beta} q_{j\beta}. \quad (26)$$

The coefficients $A_{i\alpha,j\beta}$ obey the orthonormality relations $\sum_{i,\alpha} M_i A_{i\alpha,j\beta} \times A_{i\alpha,j'\beta'} = \delta_{j\beta,j'\beta'}$. We now can solve this problem in the usual way by introducing boson creation and annihilation operators $b_{j\beta}^\dagger$ and $b_{j\beta}$ for the $(j\beta)^{\text{th}}$ mode; the creation and annihilation operators obey the commutation relation $[b_{j\beta}, b_{j'\beta'}^\dagger] = \delta_{j\beta,j'\beta'}$. With this transformation, the total ionic Hamiltonian is just the sum of the Hamiltonians for each normal mode:

$$H_{\text{ion}} = \sum_{j,\beta} (b_{j\beta}^\dagger b_{j\beta} + \frac{1}{2}) \omega_{j\beta} \quad (27)$$

Next, much like in Section , we expand the field operator for the electrons into a part that describes electrons incident from the left, and a part that describes electrons incident from the right: $\hat{\Psi} = \hat{\Psi}^{\text{L}} + \hat{\Psi}^{\text{R}}$.

We now express $H_{\text{el-ion}}$ in terms of the fermionic and bosonic creation and annihilation operators [44]:

$$H_{\text{el-ion}} = \int d\mathbf{r} \sum_i V_{\text{el-ion}}(\mathbf{r} - \mathbf{R}_i) \quad (28)$$

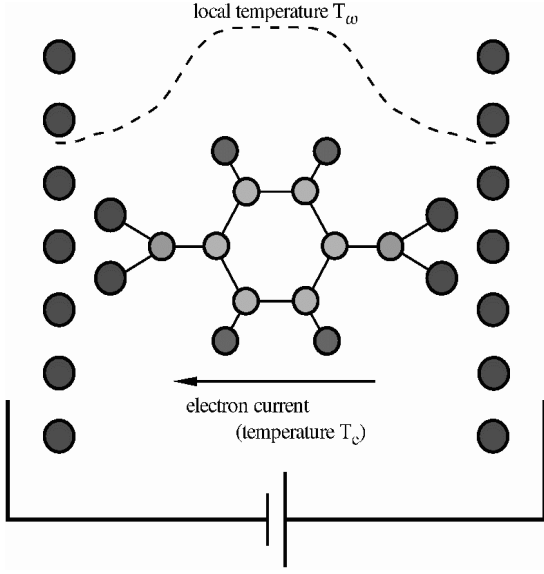


FIG. 4: Molecular junction undergoing local heating as a result of transport. The electron gas has a temperature T_e , and the phonons a temperature T_ω .

$$\begin{aligned}
 &= \int d\mathbf{r} \sum_i \mathbf{Q}_i \cdot \nabla_{\mathbf{R}} V_{\text{el-ion}}(\mathbf{r} - \mathbf{R}_i^0) \\
 &\quad + O(Q^2) \\
 &= \sum_{\varphi, \chi} \sum_{E_1, E_2} \sum_{i\alpha, j\beta \in \text{vib.}} \sqrt{\frac{1}{2\omega_{j\beta}}} \\
 &\quad \times A_{i\alpha, j\beta} J_{E_1, E_2}^{i\alpha, \varphi\chi} a_{E_1}^{\varphi\dagger} a_{E_2}^{\chi} (b_{j\beta} + b_{j\beta}^{\dagger}), \quad (30)
 \end{aligned}$$

since we have $(\mathbf{Q}_i)_\alpha = \sum_{j\beta \in \text{vib.}} A_{i\alpha, j\beta} \sqrt{\frac{1}{2\omega_{j\beta}}} (b_{j\beta} + b_{j\beta}^{\dagger})$. The electron-phonon coupling constant is given by

$$\begin{aligned}
 J_{E_1, E_2}^{i\alpha, \varphi\chi} &= \int d\mathbf{r} \int d\mathbf{K}_{\parallel} \Psi_{E_1}^{\phi*}(\mathbf{r}, \mathbf{K}_{\parallel}) \\
 &\quad \times \frac{\partial}{\partial R_\alpha} V^{\text{ps}}(\mathbf{r}, \mathbf{R}_i^0) \Psi_{E_2}^{\chi}(\mathbf{r}, \mathbf{K}_{\parallel}), \quad (31)
 \end{aligned}$$

where $V^{\text{ps}}(\mathbf{r}, \mathbf{R}_i^0)$ denotes the pseudopotential due to the i^{th} atomic core. It is interesting to note that, unlike the equilibrium case, in a current-carrying wire the electron-phonon coupling constant depends on two types of stationary states: left- and right-moving states.

We now assume that after continuous exchange of energy, both the electronic and phonon subsystems have reached a steady-state temperature and therefore assign a temperature T_e to the electron gas, and a temperature T_ω to the phonons (see schematic in figure 4), so that the statistics of the $(j\beta)^{\text{th}}$ phonon in the junction can be described by the Bose-Einstein distribution:

$$g_{j\beta} = \frac{1}{e^{\omega_{j\beta}/k_B T_\omega} - 1}, \quad (32)$$

where T_ω is the local temperature of the junction.

We can now use the Fermi's Golden Rule to infer rates of phonon emission and absorption, and thus explicitly evaluate equation (22) [44, 45, 46]. Accordingly, the composite electron-phonon system's transition rate from an initial state $|i\rangle$ to a final state $|f\rangle$ is

$$R_{j\beta} = 2\pi |\langle i | H_{\text{el-ion}}^{j\beta} | f \rangle|^2 \delta(E_f - E_i - \omega_{j\beta}). \quad (33)$$

E_i and E_f denote the energy of the electron in the initial and final state, respectively. We are only considering the transition rate for an electron interacting with the $(j\beta)^{\text{th}}$ mode, and so we have defined $H_{\text{el-ion}}^{j\beta}$ to be the $(j\beta)^{\text{th}}$ term in the $H_{\text{el-ion}}$ Hamiltonian (see equation (30)).

Let us consider the case where an electron incident from the right emits a phonon. We can evaluate the statistical average of the square of the matrix element of the Hamiltonian in equation (33) to obtain

$$\begin{aligned}
 &\langle |\langle i | H_{\text{el-ion}}^{j\beta, \text{R}, 2} | f \rangle|^2 \rangle = \\
 &\left| \sum_{i\alpha} \sqrt{\frac{1}{2\omega_{j\beta}}} A_{i\alpha, j\beta} J_{E-\omega_{j\beta}, E}^{i\alpha, \text{LR}} \sqrt{(1 + g_{j\beta}) f_E^{\text{R}} (1 - f_{E-\omega_{j\beta}}^{\text{L}})} \right|^2. \quad (34)
 \end{aligned}$$

Note that the 1 that is added to $g_{j\beta}$ corresponds to spontaneous emission.

The power emitted by right-incident electrons is simply

$$w_{j\beta}^{\text{R}, 2}(E_i, E_f) = (E_f - E_i) R_{j\beta} \quad (35)$$

$$\begin{aligned}
 &= 2\pi |\langle i | H_{\text{el-ion}}^{j\beta} | f \rangle|^2 (E_f - E_i) \\
 &\quad \times \delta(E_f - E_i - \omega_{j\beta}). \quad (36)
 \end{aligned}$$

The total power emitted by right-incident electrons to the $(j\beta)^{\text{th}}$ mode is the sum over all initial and final states:

$$W_{j\beta}^{\text{R}, 2} = 2 \sum_{E_i} \sum_{E_f} w_{j\beta}^{\text{R}, 2}(E_i, E_f) \quad (37)$$

$$\begin{aligned}
 &= 2 \sum_{E_i} \sum_{E_f} 2\pi |\langle i | H_{\text{el-ion}}^{j\beta} | f \rangle|^2 (E_f - E_i) \\
 &\quad \times \delta(E_f - E_i - \omega_{j\beta}) \quad (38)
 \end{aligned}$$

$$\begin{aligned}
 &= 2 \int dE_i D_{E_i}^{\text{R}} \int dE_f D_{E_f}^{\text{L}} 2\pi |\langle i | H_{\text{el-ion}}^{j\beta} | f \rangle|^2 \\
 &\quad \times (E_f - E_i) \delta(E_f - E_i - \omega_{j\beta}) \quad (39)
 \end{aligned}$$

$$= 4\pi \int dE_i D_{E_i}^{\text{R}} D_{E_i - \omega_{j\beta}}^{\text{L}} |\langle i | H_{\text{el-ion}}^{j\beta} | f \rangle|^2 \omega_{j\beta}, \quad (40)$$

where we have multiplied by a factor of 2 due to spin degeneracy. In taking the continuum limit, we have introduced $D_E^{\text{R(L)}}$, which is the partial density of states of electrons moving to the right (left) with energy E .

Finally, the total power emitted by right-incident electrons to the $(j\beta)^{\text{th}}$ mode is therefore

$$\begin{aligned}
 \langle W_{j\beta}^{\text{R}, 2} \rangle &= 2\pi(1 + g_{j\beta}) \int dE \left| \sum_{i\alpha} A_{i\alpha, j\beta} J_{E-\omega_{j\beta}}^{i\alpha, \text{LR}} \right|^2 \\
 &\quad \times f_E^{\text{R}} (1 - f_{E-\omega_{j\beta}}) D_E^{\text{R}} D_{E-\omega_{j\beta}}^{\text{L}}. \quad (41)
 \end{aligned}$$

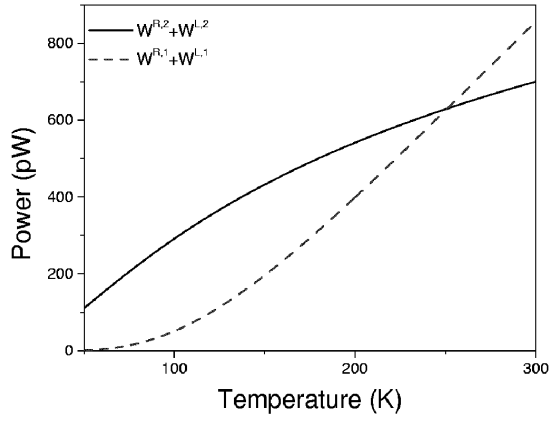


FIG. 5: Absolute magnitude of the power due to electron-phonon interactions as a function of T_ω . The intersection of the two curves gives the steady-state temperature of the junction.

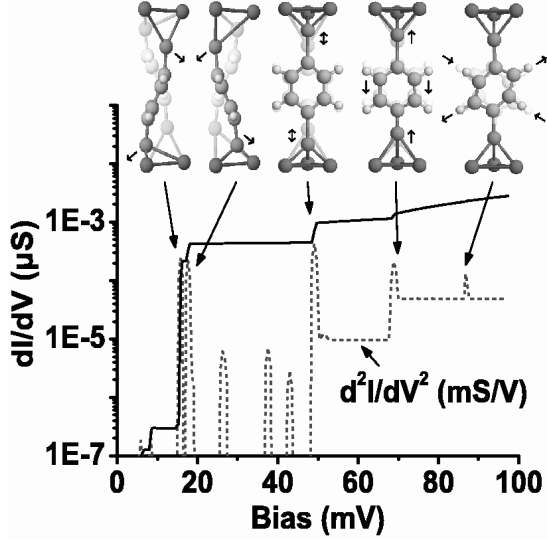


FIG. 6: Steady-state temperature as a function of applied bias for two different contact geometries: a molecular junction, and a single gold atom contact. A schematic of the contact geometry is shown as an inset for each case. For both contact geometries, the nanojunction is not in thermal contact with the bulk electrodes. Reprinted with permission from [44].

Similar considerations apply to all other processes that contribute to equation (22).

The local temperature of the junction T_ω is evaluated (at a fixed electronic temperature T_e) when the total power (22) is zero. This is illustrated in Figure 5 where the magnitude of the sum of the heating processes is plotted on the same graph as the magnitude of the sum of the cooling processes as a function of T_ω . The point where the two curves intersect is the steady-state temperature of the nanojunction.

Let us now discuss two examples. We first neglect cooling due to dissipation into the electrodes. Figure 6 shows

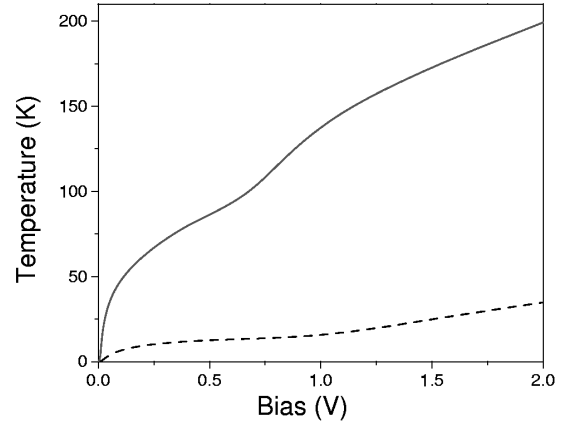


FIG. 7: Steady-state temperature as a function of applied bias for the same geometries as in Figure 6, where the dashed line corresponds to the molecular junction, and the solid line corresponds to the gold point contact. Dissipation into the bulk electrodes is taken into account. Reprinted with permission from [44].

the steady-state temperature as a function of applied bias for two different nanojunctions, a gold point contact and a molecular junction. We note that local heating occurs when a certain threshold bias is reached. This is because a given vibrational mode cannot be excited unless the incident electron is energetic enough to supply the requisite amount of energy; that is, $V_{\text{Bias}}^{(\text{crit.})} = \min\{\omega_{i\alpha}\}$. The onset bias for heating is in good agreement with experimental observations in the gold point-contact case [49]. Once the threshold bias is reached, however, the local temperature of the junction rises quickly, since cooling processes cannot effectively compensate for heating processes. Note that, in this case, very large temperatures can be reached at very small biases.

This is in contrast to Figure 7, which depicts the same process, but with an important difference: the nanojunction and contacts are now assumed to be thermally coupled with each other, i.e. energy can be dissipated into the bulk electrodes. In order to estimate this energy transfer we use the following expression for elastic phonon scattering between a bulk material A in contact with another bulk material B via a weak mechanical link (the nanojunction) [50]:

$$I_{\text{th}} = 4\pi K^2 \int d\varepsilon \varepsilon N_A(\varepsilon) N_B(\varepsilon) [g(T_A, \varepsilon) - g(T_B, \varepsilon)], \quad (42)$$

where $g(T_{A(B)}, \varepsilon)$ is the Bose-Einstein distribution at a temperature $T_{A(B)}$ and energy ε and $N_{A(B)}$ is the phonon spectral density of states of surface A(B) [50]. The weak mechanical link is modeled via a harmonic oscillator with stiffness K .

Applying equation (42) to our case we obtain the results of Figure 7 [44]. Notice that the bias scale in Figure 7 is much different than the one in Figure 6, i.e. the

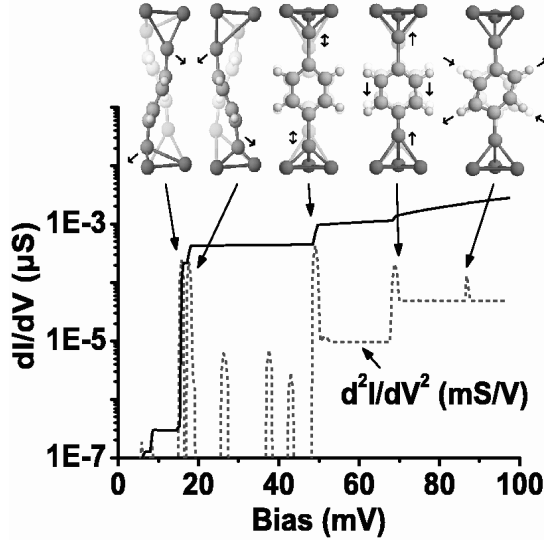


FIG. 8: Magnitude of the differential conductance through a molecular junction made of a benzene-dithiolate molecule. The dashed line gives the derivative of the differential conductance, while the insets illustrate the major longitudinal phonon modes Reprinted with permission from [54]. Copyright 2004 American Chemical Society.

majority of heat generated in the junction is dissipated into the bulk electrodes. However, in real devices poor thermal contact between the junction and the electrodes can actually occur, as can localized phonon modes within the junction which have low coupling with the continuum of modes of the bulk electrodes [46]. Such instances can lead to very large local temperatures in the junction with consequent structural instabilities [44, 46, 51]. Such instabilities have been actually observed in metallic point contacts [52] and may be responsible for the low yield in fabricating molecular junctions [53].

INELASTIC CONDUCTANCE

In addition to local heating, electron-phonon coupling can yield a lot of information on the internal structure of nanoscale junctions: discontinuities in the conductance can occur when the energy of incident electrons becomes large enough to excite different vibrational modes of the junction.

In order to calculate the inelastic current, let us consider the case of an electron incident from the right. By treating the electron-phonon interaction as a perturbation, the total wavefunctions of the (electron plus phonon) system can be written in terms of the states $|\Psi_E^R; n_{i\alpha}\rangle = |\Psi_E^R\rangle \otimes |n_{i\alpha}\rangle$. The wavefunction of the system, including electron-phonon interactions is therefore (to first order): $|\Phi_E^R; n_{i\alpha}\rangle = |\Psi_E^R; n_{i\alpha}\rangle + |\delta\Psi_E^R; n_{i\alpha}\rangle$, where $|\delta\Psi_E^R; n_{i\alpha}\rangle$ is the leading-order change in the wavefunction due to electron-phonon interaction. We can then calculate the leading correction to the total wavefunction:

$$|\delta\Psi_E^R; n_{j\beta}\rangle = \lim_{\varepsilon \rightarrow 0^+} \sum_{\phi'=L, R} \sum_{j', \beta'} \int dE' D_E^{\phi'} \times \frac{\langle \Psi_{E'}^{\phi'}; n_{j'\beta'} | H_{\text{el-ion}} | \Psi_E^R; n_{j\beta} \rangle \langle \Psi_{E'}^{\phi'}; n_{j'\beta'} |}{\varepsilon(E, n_{j\beta}) - \varepsilon(E', n_{j'\beta'}) - i\varepsilon}. \quad (43)$$

Once again, $D_E^{L(R)}$ is the partial density of states for electrons incident from the left (right). $\varepsilon(E, n_{j\beta}) = E + (n_{j\beta} + \frac{1}{2})\omega_{j\beta}$ is the energy of state $|\Psi_E^R; n_{j\beta}\rangle$. [66]

Using the identity $\lim_{\varepsilon \rightarrow 0} \frac{1}{z - i\varepsilon} = P(\frac{1}{z}) + i\pi\delta(z)$, where $P(x)$ denotes the principle value of x , together with the matrix element that leads to equation (34), we obtain

$$|\delta\Psi_E^R; n_{j\beta}\rangle = i\pi \sum_{i\alpha} \sqrt{\frac{1}{2\omega_{j\beta}}} A_{i\alpha, j\beta} \left[D_{E+\omega_{j\beta}}^L \sqrt{g_{j\beta} f_E^R (1 - f_{E+\omega_{j\beta}}^L)} J_{E+\omega_{j\beta}}^{i\alpha, LR} |\Psi_{E+\omega_{j\beta}, E}^L; n_{j\beta} - 1\rangle + D_{E-\omega_{j\beta}}^L \sqrt{(1 + g_{j\beta}) f_E^R (1 - f_{E-\omega_{j\beta}}^L)} J_{E-\omega_{j\beta}}^{i\alpha, LR} |\Psi_{E-\omega_{j\beta}, E}^L; n_{j\beta} + 1\rangle \right] \quad (44)$$

The analogous expression for $|\delta\Psi_E^L; n_{j\beta}\rangle$ is obtained by simply interchanging all R's with L's.

As an example let us assume that the electronic temperature T_e is equal to zero. In that case, for an external bias $V = E_{\text{FL}} - E_{\text{FR}}$, only normal modes with energies $\omega_{j\beta} < V$ can be excited. (Again, we are assuming the left electrode is positively biased.) Furthermore, if we assume negligible local heating, and that the few excited phonons

decay on a short time scale, then we have $g_{j\beta} = 0$. In this case, the inelastic contribution to the current is:

$$\delta I = -i \int_{E_{\text{FL}}}^{E_{\text{FR}}} dE \int d\mathbf{R} \int d\mathbf{K}_{\parallel} [(\delta\Psi_E^R)^* \partial_z \delta\Psi_E^R - \partial_z (\delta\Psi_E^R)^* \delta\Psi_E^R]. \quad (45)$$

In Figure 8 we plot the inelastic conductance of a molecular junction. It is evident that only specific modes

with large longitudinal component (with respect to the direction of current flow) dominate the inelastic conductance, while modes with large transverse component contribute negligibly. In addition, it is shown in Ref. [54] that inelastic current-voltage characteristics are quite sensitive to the structure of the contact between the molecule and the electrodes thus providing a powerful tool to extract the bonding geometry in molecular wires.

CONCLUSIONS

We have presented a review of several current-induced effects in nanoscale conductors and their description at the atomic level. These effects provide a wealth of information on the transport properties of atomic and molecular junctions beyond the value of the average current. In addition, their understanding is paramount to the possible application of nanoscale systems in electronics.

One of us (MD) is indebted to the students and research associates who have worked with him over the past years on the issues described in this review: M. Zwolak, J. Lagerqvist, Y.-C. Chen, M. Chshiev and Z. Yang. We are also thankful for illuminating discussions with N.D. Lang and T.N. Todorov. We acknowledge support from the NSF Grant No. DMR-01-33075.

* Electronic address: bushong@physics.ucsd.edu

† Electronic address: diventra@physics.ucsd.edu

- [1] M. Di Ventra, S. Evoy, J.R. Heflin: *Introduction to Nanoscale Science and Technology* (Kluwer Academic Publishers, Boston, 2004)
- [2] M. Di Ventra, T.N. Todorov: Transport in nanoscale systems: the microcanonical versus grand-canonical picture, *J. Phys.-Condens. Matter* **16**, 8025–8034 (2004)
- [3] A.P. Horsfield, D.R. Bowler, A.J. Fisher, T.N. Todorov, M.J. Montgomery: Power dissipation in nanoscale conductors: classical, semi-classical and quantum dynamics, *J. Phys.-Condens. Matter* **16**, 3609–3622 (2004)
- [4] H. Ohnishi, Y. Kondo, K. Takayanagi: Quantized conductance through individual rows of suspended gold atoms, *Nature* **395**, 780 (1998)
- [5] A. Yazdani, D.M. Eigler, N.D. Lang: Off-resonance conduction through atomic wires, *Science* **272**, 1921 (1996)
- [6] V. Rodrigues, D. Ugarte: Real-time imaging of atomistic process in one-atom-thick metal junctions, *Phys. Rev. B* **63**, 073 405 (2001)
- [7] R.M. Metzger, B. Chen, U. Höpfner, M.V. Lakshmikantham, D. Vuillaume, T. Kawai, X. Wu, H. Tachibana, T.V. Hughes, H. Sakurai, J.W. Baldwin, C. Hosch, M.P. Cava, L. Brehmer, G.J. Ashwell: Unimolecular electrical rectification in hexadecylquinolinium tricyanoquinodimethanide, *J. Am. Chem. Soc.* **119**, 10 455–10 466 (1997)
- [8] C. Zhou, M.R. Deshpande, M.A. Reed, L.J. II, J.M. Tour: Nanoscale metal/self-assembled monolayer/metal heterostructures, *Appl. Phys. Lett.* **71**, 611–613 (1997)
- [9] M.A. Reed, C. Zhou, C.J. Muller, T.P. Burgin, J.M. Tour: Conductance of a molecular junction, *Science* **278**, 252–254 (1997)
- [10] S. Datta, W. Tian, S. Hong, R. Reifenberger, J. Henderson, C.P. Kubiak: Current-voltage characteristics of self-assembled monolayers by scanning tunneling microscopy, *Phys. Rev. Lett.* **79**, 2530–2533 (1997)
- [11] J. Gimzewski, C. Joachim: Nanoscale science of single molecules using local probes, *Science* **283**, 1683–1688 (1999)
- [12] J. Chen, M.A. Reed, A.M. Rawlett, J.M. Tour: Large on-off ratios and negative differential resistance in a molecular electronic device, *Science* **286**, 1550–1552 (1999)
- [13] M.A. Reed, J. Chen, A.M. Rawlett, D.W. Price, J.M. Tour: Molecular random access memory cell, *Appl. Phys. Lett.* **78**, 3735–3737 (2001)
- [14] N.D. Lang, P. Avouris: Carbon-atom wires: Charge-transfer doping, voltage drop, and the effect of distortions, *Phys. Rev. Lett.* **84**, 358–361 (2000)
- [15] M. Di Ventra, N.D. Lang: Transport in nanoscale conductors from first principles, *Phys. Rev. B* **65**, 045 402 (2002)
- [16] J. Tomfohr, G. Ramachandran, O.F. Sankey, S.M. Lindsay: in *Introducing Molecular Electronics*, ed. by G. Cuniberti, G. Fagas, K. Richter (Springer, New York, 2005), Lecture Notes in Physics; *in print*
- [17] A. Messiah: *Quantum Mechanics* (Dover Publications, Inc., New York, 1999)
- [18] N. Sai, M. Zwolak, G. Vignale, M. Di Ventra: Non-local corrections to the DFT-LDA electron conductance in nanoscale systems, cond-mat/0411098 (2004)
- [19] Z. Yang, A. Tackett, M. Di Ventra: Variational and non-variational principles in quantum transport calculations, *Phys. Rev. B* **66**, 041 405(R) (2002)
- [20] N.D. Lang: Field-induced transfer of an atom between two closely spaced electrodes, *Phys. Rev. B* **45**, 13 599–13 606 (1992)
- [21] N.D. Lang: Erratum: Field-induced transfer of an atom between two closely spaced electrodes, *Phys. Rev. B* **51**, 2029(E) (1995)
- [22] N.D. Lang: Bias-induced transfer of an aluminum atom in the scanning tunneling microscope, *Phys. Rev. B* **49**, 2067–2071 (1994)
- [23] N.D. Lang: Resistance of atomic wires, *Phys. Rev. B* **52**, 5335–5342 (1995)
- [24] J. Jortner, A. Nitzan, M.A. Ratner: in *Introducing Molecular Electronics*, ed. by G. Cuniberti, G. Fagas, K. Richter (Springer, New York, 2005), Lecture Notes in Physics; *in print*
- [25] P. Hänggi, S. Kohler, J. Lehmann, M. Strass: in *Introducing Molecular Electronics*, ed. by G. Cuniberti, G. Fagas, K. Richter (Springer, New York, 2005), Lecture Notes in Physics; *in print*
- [26] K. Stokbro, J. Taylor, M. Brandbyge, H. Guo: in *Introducing Molecular Electronics*, ed. by G. Cuniberti, G. Fagas, K. Richter (Springer, New York, 2005), Lecture Notes in Physics; *in print*
- [27] A. Di Carlo, A. Pecchia, L. Latessa, T. Frauenheim, G. Seifert: in *Introducing Molecular Electronics*, ed. by

- G. Cuniberti, G. Fagas, K. Richter (Springer, New York, 2005), Lecture Notes in Physics; *in print*
- [28] R. Landauer: Conductance from transmission: Common sense points, *Physica Scripta* **T42**, 110–114 (1992)
- [29] R. Landauer: Electrical transport in open and closed systems, *Zeitschrift für Physik B– Condensed Matter* **68**, 217–228 (1987)
- [30] J. Lagerqvist, Y.C. Chen, M. Di Ventra: Shot noise in parallel wires, *Nanotechnology* **15**, S459–S464(1) (2004)
- [31] M. Di Ventra, S. Pantelides: Hellmann-feynman theorem and the definition of forces in quantum time-dependent and transport problems, *Phys. Rev. B* **61**, 16 207 (2000)
- [32] T. Seideman: Current-driven dynamics in molecular-scale devices, *J. Phys.-Condens. Matter* **15**, R521–R549 (2003)
- [33] M. Di Ventra, Y.C. Chen, T.N. Todorov: Are current-induced forces conservative?, *Phys. Rev. Lett.* **92**, 176 803 (2004)
- [34] Z. Yang, M. Di Ventra: Nonlinear current-induced forces in Si atomic wires, *Phys. Rev. B* **67**, 161 311(R) (2003)
- [35] T.N. Todorov: Time-dependent tight binding, *J. Phys.-Condens. Matter* **13**, 10 125–10 148 (2001)
- [36] M. Di Ventra, S. Pantelides, N. Lang: Current-induced forces in molecular wires, *Phys. Rev. Lett.* **88**, 046 801 (2002)
- [37] M. Di Ventra, N.D. Lang, S. Pantelides: Electronic transport in single molecules, *Chem. Phys.* **281**, 189 (2002)
- [38] Y.M. Blanter, M. Büttiker: Shot noise in mesoscopic conductors, *Physics Reports* **336**, 1–166 (2000)
- [39] Y.C. Chen, M. Di Ventra: Shot noise in nanoscale conductors from first principles, *Phys. Rev. B* **67**, 1553 304 (2003)
- [40] S. Camalet, J. Lehmann, S. Kohler, P. Hänggi: Current noise in ac-driven nanoscale conductors, *Phys. Rev. Lett.* **90**, 210 602 (2003)
- [41] R. Kubo, M. Toda, N. Hashitsume: *Statistical Physics II: Nonequilibrium Statistical Mechanics* (Springer, New York, 1992)
- [42] W. Schottky: Über spontane stromschwankungen in verschiedenen elektrizitätsleitern, *Annals of Physics* **57**, 541 (1918)
- [43] N.D. Lang: Anomalous dependence of resistance on length in atomic wires, *Phys. Rev. Lett.* **79**, 1357–1360 (1997)
- [44] Y.C. Chen, M. Zwolak, M. Di Ventra: Local heating in nanoscale conductors, *Nano Lett.* **3**, 1691 (2003)
- [45] M.J. Montgomery, T.N. Todorov, A.P. Sutton: Power dissipation in nanoscale conductors, *J. Phys.-Condens. Matter* **14**, 5377–5389 (2002)
- [46] M.J. Montgomery, T.N. Todorov: Electron-phonon interaction in atomic-scale conductors: Einstein oscillators versus full phonon modes, *J. Phys.-Condens. Matter* **15**, 8781–8795 (2003)
- [47] D. Segal, A. Nitzan, W.B. Davis, M.R. Wasielewski, M.A. Ratner: Electron transfer rates in bridged molecular systems 2: A steady-state analysis of coherent tunneling and thermal transitions, *J. Phys. Chem. B* **104**, 3817–3829 (2000)
- [48] A. Troisi, M.A. Ratner, A. Nitzan: Vibronic effects in off-resonant molecular wire conduction, *J. Chem. Phys.* **118**, 6072–6082 (2003)
- [49] N. Agraït, C. Untiedt, G. Rubio-Bollinger, S. Vieira: Onset of energy dissipation in ballistic atomic wires, *Phys. Rev. Lett.* **88**, 216 803 (2002)
- [50] K.R. Patton, M.R. Geller: Thermal transport through a mesoscopic weak link, *Phys. Rev. B* **64**, 155 320 (2001)
- [51] Z. Yang, M. Chshiev, M. Zwolak, Y. Chen, M. Di Ventra: Role of heating and current-induced forces in the stability of atomic wires, *Phys. Rev. B* **71**, 041 402(R) (2005)
- [52] R.H.M. Smit, C. Untiedt, J.M. van Ruitenbeek: The high-bias stability of monatomic chains, *Nanotechnology* **15**, S472–S478 (2004)
- [53] N.B. Zhitenev, A. Erbe, Z. Bao: Single- and multigrain nanojunctions with a self-assembled monolayer of conjugated molecules, *Phys. Rev. Lett.* **92**, 186 805 (2004)
- [54] Y. Chen, M. Zwolak, M. Di Ventra: Inelastic current-voltage characteristics of atomic and molecular junctions, *Nano Letters* **4**, 1709–1712 (2004)
- [55] D.M. Ceperley, B. Alder: Ground state of the electron gas by a stochastic method, *Phys. Rev. Lett.* **45**, 566 (1980)
- [56] J.P. Perdew, A. Zunger: Self-interaction correction to density-functional approximations for many-electron systems, *Phys. Rev. B* **23**, 5048 (1981)
- [57] S.S. Sorbello: *Solid State Physics*, Vol. 51 (Academic Press, Inc., New York, 1998)
- [58] M. Büttiker: Scattering theory of thermal and excess noise in open conductors, *Phys. Rev. Lett.* **65**, 2901–2904 (1990)
- [59] For the detailed implementation of the approach outlined in this work see the original papers [14, 15].
- [60] One possible choice of exchange-correlation functional is the one given in [55], as parametrized in [56]. For an extended discussion of the local density approximation, see reference [27].
- [61] For other examples of calculations using different basis sets, see Section 2.2 of reference [26], and the references therein.
- [62] Note that this definition of “direct force”, and corresponding “wind force”, is not universal in literature. For a discussion of the various definitions, see reference [57].
- [63] The presence of the nanojunction causes \mathbf{K}_{\parallel} to cease to be a good quantum number; we still use it here as a “label” to enumerate scattering states.
- [64] As for the current, this expression can be reduced to the well-known result $S = \frac{V_B}{\pi} \sum_n T_n (1 - T_n)$ [58] if the transmission probabilities T_n of each mode are extracted from the scattering wavefunctions; see reference [30].
- [65] We assume here that at those biases when current-induced forces are large heating is small. This is generally true if dissipation into the bulk electrodes is efficient [51].
- [66] Since the electron-phonon coupling is small for the systems considered here, we assume the energy E is the unperturbed electronic energy, i.e. the elastic correction to the electronic energy is negligible.